Materials Chemistry and Physics 132 (2012) 223–227

Contents lists available at SciVerse ScienceDirect

Materials Chemistry and Physics

journal homepage: www.elsevier.com/locate/matchemphys

Synthesis and electrochemical properties of nanorod-shaped $LiMn_{1.5}Ni_{0.5}O_4$ cathode materials for lithium-ion batteries

Seo Hee Ju [a], Yun Chan Kang [b], Yang-Kook Sun [c], Dong-Won Kim [a,*]

[a] Department of Chemical Engineering, Hanyang University, 17 Haedang-dong, Seongdong-gu, Seoul 133-791, Republic of Korea
[b] Department of Chemical Engineering, Konkuk Universuty, 1 Hwayang-dong, Gwangjin-gu, Seoul 143-701, Republic of Korea
[c] Department of Energy Engineering, Hanyang University, 17 Haedang-dong, Seongdong-gu, Seoul 133-791, Republic of Korea

ARTICLE INFO

Article history:
Received 22 April 2011
Received in revised form 1 November 2011
Accepted 20 November 2011

Keywords:
Oxides
Nanostructures
Chemical synthesis
Electrochemical properties

ABSTRACT

Nanorod-shaped $LiMn_{1.5}Ni_{0.5}O_4$ cathode powders were synthesized by a co-precipitation method with oxalic acid. Their structures and electrochemical properties were characterized by SEM, XRD and galvanostatic charge–discharge tests. The resulting nanorod-shaped $LiMn_{1.5}Ni_{0.5}O_4$ cathode active materials delivered a specific discharge capacity of 126 mAh g^{-1} at 0.1 C rate. These active materials exhibited better capacity retention and higher rate performance than those of $LiMn_{1.5}Ni_{0.5}O_4$ cathode powders with irregular morphology.

1. Introduction

$LiMn_2O_4$ materials have been studied as substitutes for $LiCoO_2$ materials because of their economical and environmental advantages. However, $LiMn_2O_4$ materials are susceptible to capacity fading upon prolonged cycling. Therefore, the synthesis of $LiMn_2O_4$ materials with stable cycle performance is required [1–3]. Many research groups reported that transition metal-substituted spinel materials ($LiMn_{2-x}M_xO_4$, M = Cr, Co, Fe, Ni) could suppress Jahn–Teller distortion, which has been one of the most important causes for capacity fading of spinel $LiMn_2O_4$ materials [4,5]. The electrochemical properties of $LiMn_{2-x}M_xO_4$ active materials depend strongly on the kinds of transition metals and their concentrations [6–9]. Among these materials, $LiMn_{1.5}Ni_{0.5}O_4$ active materials exhibit good electrode performance. The electrochemical performances of these materials are strongly affected by the physical properties of cathode powders such as morphology, particle size, specific surface area and crystallinity.

Recently, many research groups have demonstrated significantly improved capacity in electrodes prepared from nanocrystalline active materials in comparison with electrodes comprised of micro-sized particles [10–12]. Nano-sized cathode materials have high surface area, and accordingly, faster charge transfer kinetics of Li^+ ions. Various liquid solution methods such as sol–gel, molten salt, co-precipitation and composition emulsion drying have been applied to the preparation of nano-sized cathode particles. The co-precipitation method is known to be a simple route to prepare fine, well-crystallized, high purity and homogeneous powders of single or multi-component oxides [13–17]. In the present study, nanorod-shaped $LiMn_{1.5}Ni_{0.5}O_4$ cathode powders were prepared by the co-precipitation method with oxalic acid. The morphology of $LiMn_{1.5}Ni_{0.5}O_4$ cathode powders could be controlled to nanorod-shaped one by changing the quantity of the oxalic acid. The effects of the ratio of oxalic acid to metal on the characteristics of $LiMn_{1.5}Ni_{0.5}O_4$ cathode powders were investigated.

2. Experimental

$LiMn_{1.5}Ni_{0.5}O_4$ cathode powders were synthesized by co-precipitation using oxalic acid. A stoichiometric amount of lithium acetate dehydrate [$Li(CH_3COO)\cdot 2H_2O$, Aldrich], manganese (II) acetate tetrahydrate [$Mn(CH_3COO)_2\cdot 4H_2O$, Aldrich] and nickel (II) acetate tetrahydrate [$Ni(CH_3COO)_2\cdot 4H_2O$, Aldrich] were dissolved in de-ionized water. The solution was stirred continuously under heating at 60 °C. The oxalic acid solution was added to the homogeneous solution drop by drop. The mole ratio of oxalic acid to metal was changed from 0.1 to 5.0. The solution was stirred further at 90 °C. The precipitate solution was dried overnight at 110 °C. The dried precipitate was preheated at 450 °C for 3 h to decompose the organic components. The precursor powders were annealed at 750 °C for 15 h in an air atmosphere. The morphological characteristics of the powders were investigated using scanning electron microscopy (SEM, JEOL JSM 6701). The crystal structures of the $LiMn_{1.5}Ni_{0.5}O_4$ powders were investigated

* Corresponding author. Tel.: +82 2 2220 2337; fax: +82 2 2298 4101.
E-mail address: dongwonkim@hanyang.ac.kr (D.-W. Kim).

0254-0584/$ – see front matter © 2011 Elsevier B.V. All rights reserved.
doi:10.1016/j.matchemphys.2011.11.042

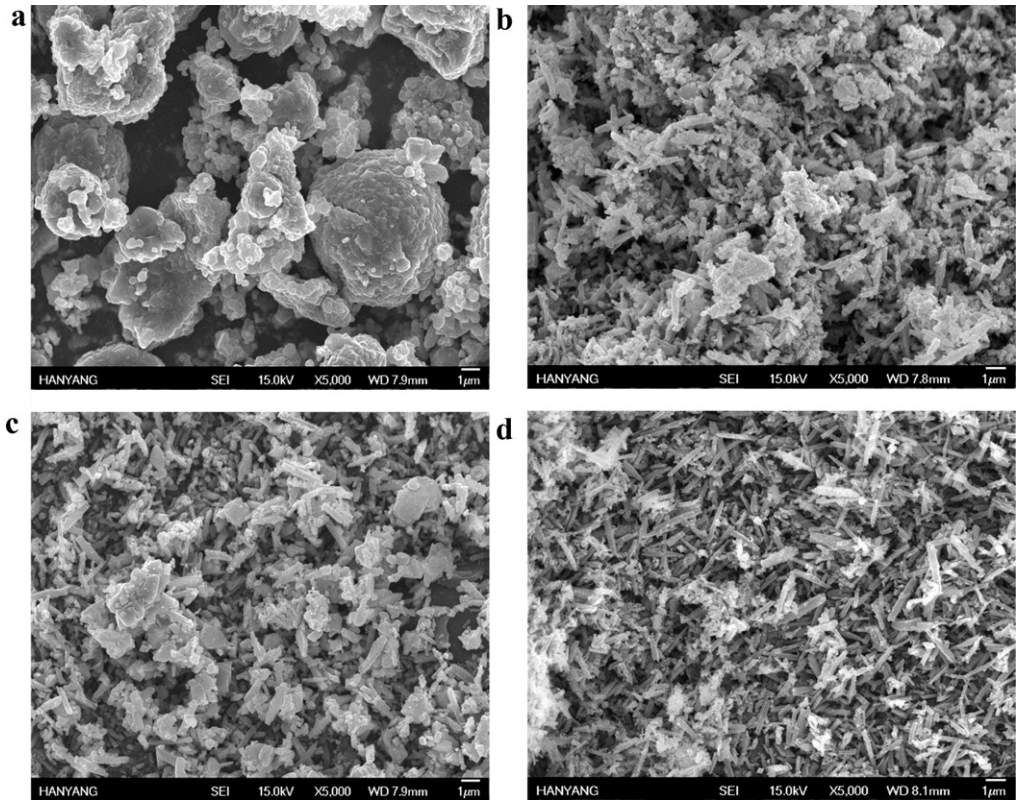

Fig. 1. SEM images of $LiMn_{1.5}Ni_{0.5}O_4$ powders obtained using different mole ratios of oxalic acid to metal. (a) 0.1, (b) 1.0, (c) 2.0, and (d) 5.0.

using X-ray diffractometry (XRD, Philips X'PERT MPD). The compositions of the $LiMn_{1.5}Ni_{0.5}O_4$ powders were analyzed using energy dispersive X-ray (EDAX). The cathode was prepared by coating the N-methyl pyrrolidone (NMP)-based slurry containing $LiMn_{1.5}Ni_{0.5}O_4$, poly(vinylidene fluoride) (PVdF) and super-P carbon (85:7.5:7.5 by weight) on an aluminum foil. The thicknesses of the electrodes ranged from 50 to 55 μm after roll pressing, and their active mass loading corresponded to a capacity of about 2.5 mAh cm^{-2}. The liquid electrolyte was 1 M $LiPF_6$ in ethylene carbonate (EC)/dimethyl carbonate (DMC) (1:1 by volume, battery grade, Techno Semichem Co., Ltd.). The lithium electrode consisted of a 150 μm-thick lithium foil that was pressed onto a copper current collector. A CR2032-type coin cell composed of lithium anode, a polypropylene separator (Celgard 2400) and $LiMn_{1.5}Ni_{0.5}O_4$ cathode was assembled with an electrolyte solution. All cells were assembled in a dry box filled with argon gas. Charge and discharge cycling tests of the Li/$LiMn_{1.5}Ni_{0.5}O_4$ cells were conducted at different current density over a voltage range of 3.0–4.9 V with battery testing equipment. The electrochemical behavior of $LiMn_{1.5}Ni_{0.5}O_4$

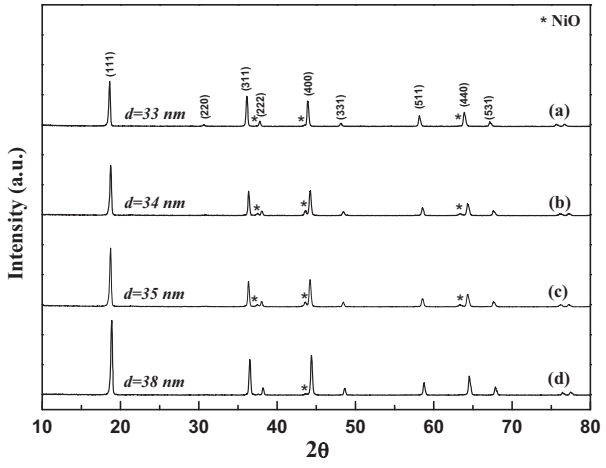

Fig. 2. XRD patterns of $LiMn_{1.5}Ni_{0.5}O_4$ powders prepared using different mole ratios of oxalic acid to metal. (a) 0.1, (b) 1.0, (c) 2.0, and (d) 5.0.

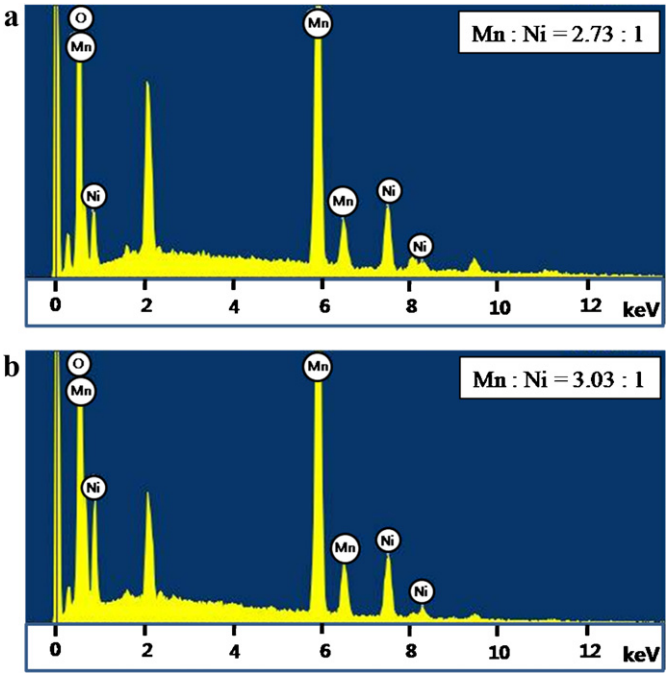

Fig. 3. EDAX spectra of $LiMn_{1.5}Ni_{0.5}O_4$ powders prepared using different mole ratios of oxalic acid to metal. (a) 0.1 and (b) 5.0.

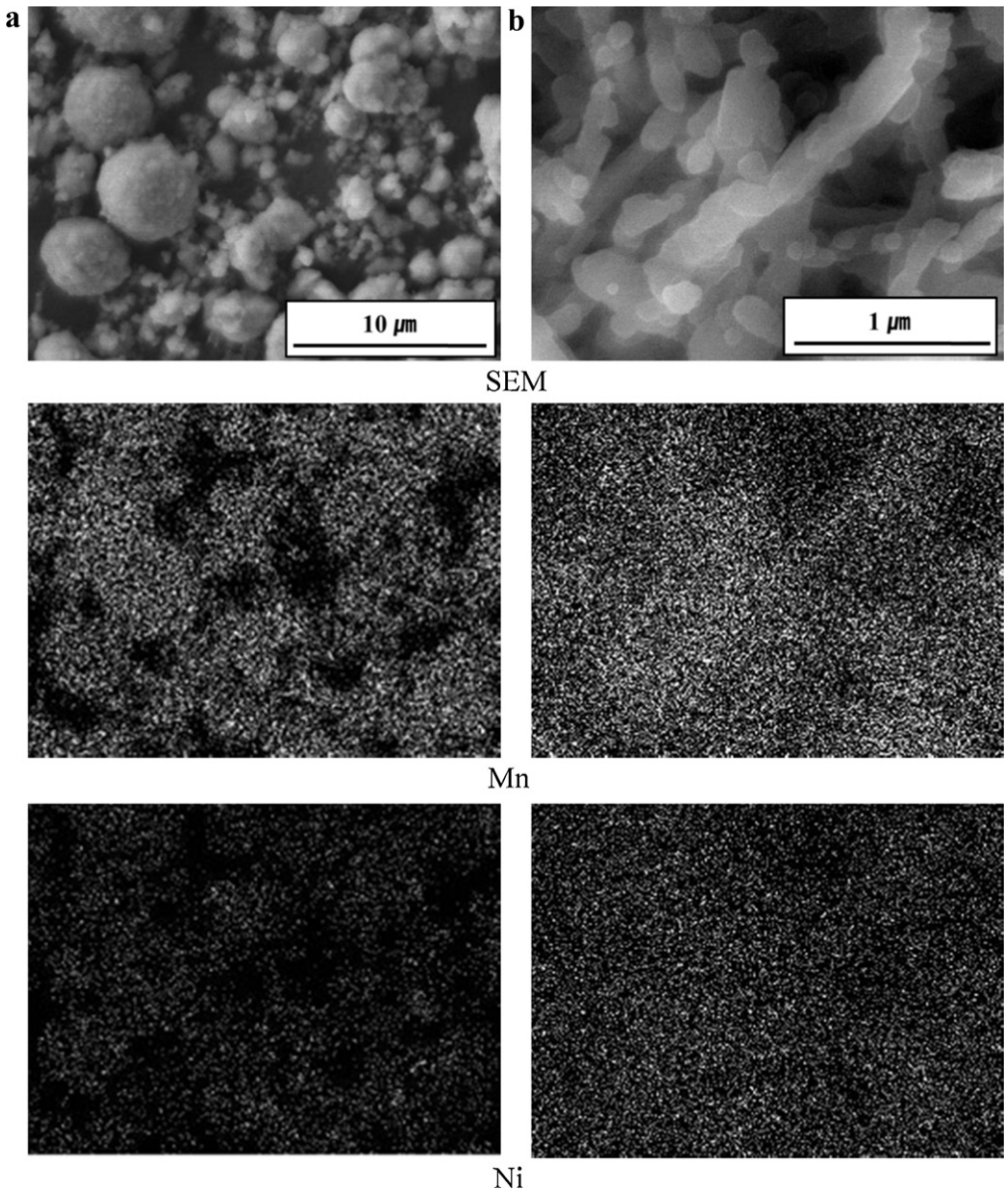

Fig. 4. Dot mappings of $LiMn_{1.5}Ni_{0.5}O_4$ powders prepared using different mole ratios of oxalic acid to metal. (a) 0.1 and (b) 5.0.

powder with different morphology was analyzed by cyclic voltammetry. The voltammograms were obtained between 3.5 and 5.0 V at a scan rate of 0.1 mV s^{-1}.

3. Results and discussion

The morphologies of the $LiMn_{1.5}Ni_{0.5}O_4$ powders obtained from the co-precipitation method with different mole ratios of oxalic acid to metal are shown in Fig. 1. The $LiMn_{1.5}Ni_{0.5}O_4$ powders prepared from the mole ratio of 0.1 exhibited irregular morphologies with a broad size distribution. As the ratio of oxalic acid to metal increased, the morphologies of the $LiMn_{1.5}Ni_{0.5}O_4$ powders became rod shaped. The $LiMn_{1.5}Ni_{0.5}O_4$ powders prepared from materials with a ratio of oxalic acid to metal of 5.0 showed smaller size and a more homogeneous distribution than $LiMn_{1.5}Ni_{0.5}O_4$ powders prepared by the ratio of oxalic acid to metal of 1.0 or 2.0. This result indicates that the quantity of the oxalic acid is important for controlling the morphology of $LiMn_{1.5}Ni_{0.5}O_4$ cathode powders. The oxalic acid acts as an organic additive during decomposition of the metal complexes at annealing process. It is oxidized with evolution of large amount of gas, and the gas evolution may help break down large agglomerated particles and inhibit the continuous growth of the powder. When the ratio of oxalic acid to metal was 5.0, the $LiMn_{1.5}Ni_{0.5}O_4$ powders were nanorod-shaped with a uniform diameter of about 150 nm and a length of 1–2 μm.

Fig. 2 shows the XRD patterns of the $LiMn_{1.5}Ni_{0.5}O_4$ cathode powders annealed at 750 °C, which were obtained via co-precipitation with different mole ratio of oxalic acid to metal. It is well known that $LiMn_{1.5}Ni_{0.5}O_4$ cathode powders show the cubic spinel (*Fd3m*) phase in which Li atoms occupy tetragonal 8a sites, Mn atoms and Ni atoms reside in octahedral 16d sites and O in 32e sites [18]. The crystal structures of $LiMn_{1.5}Ni_{0.5}O_4$ powders synthesized in this study had main crystal structures of spinel $LiMn_{1.5}Ni_{0.5}O_4$ along with a small amount of NiO peaks as minor impurities near the (3 1 1), (4 0 0) and (4 4 0) peaks. The crystallite size was calculated for each sample from the powder X-ray diffraction pattern according to Sherrer's equation [19]. The crystallite sizes of the powders were estimated from (1 1 1) peaks. The crystallite size of the $LiMn_{1.5}Ni_{0.5}O_4$ powder increased from 33 to 38 nm

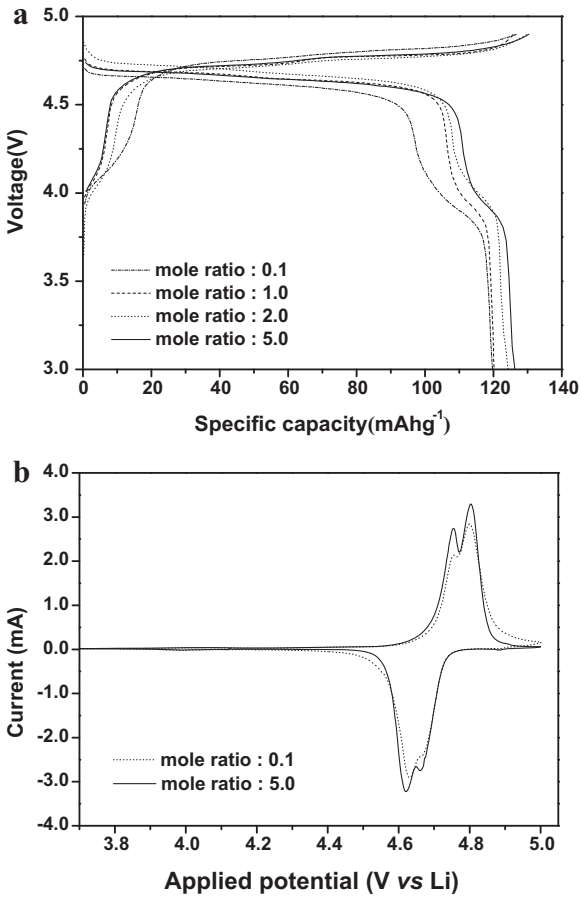

Fig. 5. (a) Initial charge and discharge curves of the $LiMn_{1.5}Ni_{0.5}O_4$ active cathode materials (room temperature, 0.1 C rate, cut-off voltage: 3.0–4.9 V), and (b) cyclic voltammograms of the $LiMn_{1.5}Ni_{0.5}O_4$ electrodes with irregular and nanorod-shaped morphology (scan rate: 0.1 mV s^{-1}).

when the mole ratio of oxalic acid to metal was increased from 0.1 to 5.0.

To analyze the chemical composition of the $LiMn_{1.5}Ni_{0.5}O_4$ powders, EDAX analysis and dot mapping were performed. Fig. 3 shows the EDAX spectrum of the $LiMn_{1.5}Ni_{0.5}O_4$ powders prepared by the ratio of oxalic acid to metal of 0.1 and 5.0. In the EDAX spectrum, the mole ratio of manganese and nickel component could be determined. The average ratio of Mn and Ni component of the $LiMn_{1.5}Ni_{0.5}O_4$ powders with irregular morphologies (oxalic acid/metal ratio was 0.1) was about 2.73:1. On the other hand, the mole ratio of Mn and Ni component of the $LiMn_{1.5}Ni_{0.5}O_4$ powders with rod-shaped morphologies (oxalic acid/metal ratio was 5.0) was about 3.03:1, which is well consistent with chemical composition of the $LiMn_{1.5}Ni_{0.5}O_4$ powders. Fig. 4 shows the results of dot mapping of the $LiMn_{1.5}Ni_{0.5}O_4$ powders prepared from the mole ratio of 0.1 and 5.0, respectively. It is found that Mn and Ni components are well dispersed inside the submicron-sized powders and rod-shaped powders. This result indicates that the $LiMn_{1.5}Ni_{0.5}O_4$ powders with homogeneous compositions can be prepared by co-precipitation method.

Fig. 5(a) compares the initial charge and discharge curves of the $LiMn_{1.5}Ni_{0.5}O_4$ cathode powders prepared with a different mole ratio of oxalic acid to metal. All of the cells showed flat discharge plateaus in the range of 4.6 to at 4.8 V *vs.* Li/Li^+, which corresponded to the oxidation of Ni^{2+} to Ni^{4+}. High mole ratios of oxalic acid to metal resulted in an increase of the discharge capacity for $LiMn_{1.5}Ni_{0.5}O_4$ materials. The initial discharge capacity of the $LiMn_{1.5}Ni_{0.5}O_4$ active cathode material obtained from

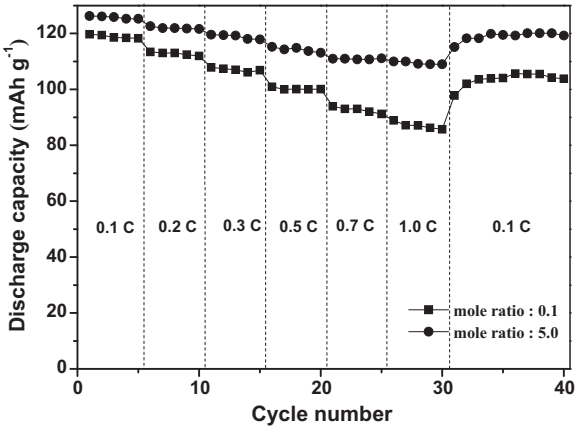

Fig. 6. Cycling performance of $LiMn_{1.5}Ni_{0.5}O_4$ cathode materials prepared when the mole ratios of oxalic acid to metal were (a) 0.1 and (b) 5.0. The C-rate was increased from 0.1 to 1.0 C after every 5 cycles and the cells were cycled again at 0.1 C rate.

the mole ratio of oxalic acid to metal of 0.1 was 119 mAh g^{-1} at a constant current density of 0.1 C rate. In contrast, the initial discharge capacity of $LiMn_{1.5}Ni_{0.5}O_4$ with a high mole ratio of oxalic acid (5.0) was 126 mAh g^{-1}. Faster kinetics is expected in the nanorod-shaped $LiMn_{1.5}Ni_{0.5}O_4$ with smaller particle size because the diffusion length for the Li^+ ions is shorter. Although the initial discharge capacity of this material is lower than theoretical one, the value is not lower as compared to those reported in the early literatures [16,17,20,21]. Fig. 5(b) shows cyclic voltammograms of the $LiMn_{1.5}Ni_{0.5}O_4$ electrodes with irregular (oxalic acid/metal ratio was 0.1) and nanorod-shaped morphology (oxalic acid/metal ratio was 5.0), respectively. These voltammograms show that these electrodes have very low redox activity around 4.0 V, which relates to the Mn^{3+}/Mn^{4+} couple, and pronounced two redox peaks between 4.5 and 4.8 V corresponded to the Ni^{2+}/Ni^{3+} and the Ni^{3+}/Ni^{4+} couples, respectively. These voltammograms are in good agreement with those reported in the previous literature [4,22,23].

Fig. 6 shows the discharge capacities of the $LiMn_{1.5}Ni_{0.5}O_4$ cathode powders with irregular and nanorod-shaped morphology with C-rate increasing from 0.1 to 1.0 C every 5 cycles. After 5 cycles at a 1.0 C rate, the cells were cycled again at a rate of 0.1 C. The $LiMn_{1.5}Ni_{0.5}O_4$ cathode powders with irregular morphology showed poor cycling performance at a high current density. The first discharge capacity dropped from 119 to 88 mAh g^{-1}, when the current densities were increased from 0.1 to 1.0 C. In contrast, nanorod-shaped $LiMn_{1.5}Ni_{0.5}O_4$ cathode powders showed better cycling performance. The active material delivered the first discharge capacity of 126, 123, 120, 115, 111 and 110 mAh g^{-1} when the current densities were increased from 0.1 to 1.0 C. After 30 cycles with different current densities, the cell recovered 94% of the first discharge capacity at a 0.1 C rate. The improved rate capabilities of the $LiMn_{1.5}Ni_{0.5}O_4$ cathode powders are believed to be due to nanorod morphology with a thickness of 150 nm that enables effective Li^+ diffusion.

Fig. 7(a) and (b) shows the discharge capacities of $LiMn_{1.5}Ni_{0.5}O_4$ cathode materials with different morphologies, which were obtained at the different rates of 0.5 C and 2 C rate, respectively. As shown in Fig. 7(a), the $LiMn_{1.5}Ni_{0.5}O_4$ cathode materials with irregular and nanorod shape morphology exhibited an initial discharge capacity of 104 and 117 mAh g^{-1}, respectively, at 0.5 C rate. Their capacity retentions were 90 and 95% after 50 cycles. At 2.0 C rate, the nanorod-shaped $LiMn_{1.5}Ni_{0.5}O_4$ cathode materials also had better cycling performance in terms of initial discharge capacity and capacity retention, as compared to those of $LiMn_{1.5}Ni_{0.5}O_4$ cathode materials with irregular shape, as presented in Fig. 7(b). Thus,

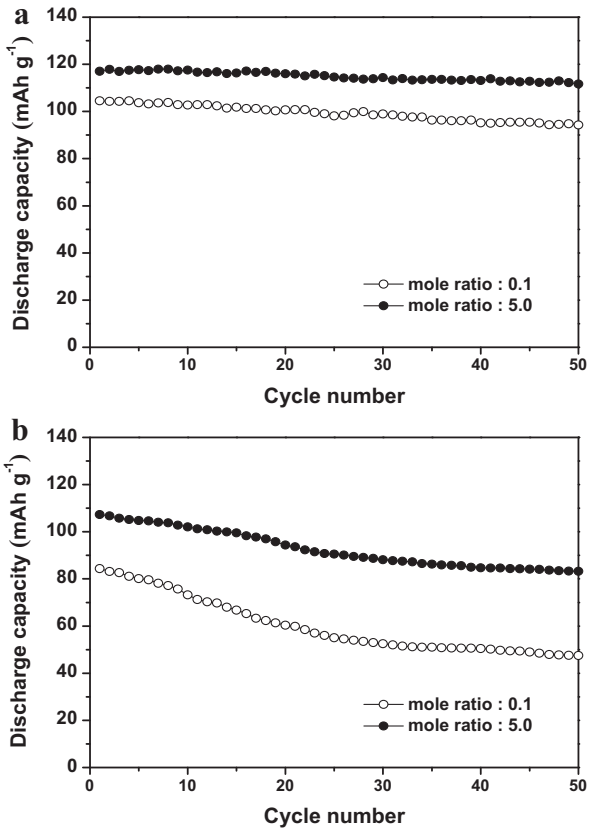

Fig. 7. Discharge capacities of $LiMn_{1.5}Ni_{0.5}O_4$ cathode materials with irregular and nanorod-shaped morphology. Cycling was carried out between 3.0 and 4.9 V at 25 °C at different current rate of (a) 0.5 C and (b) 2 C.

it can be concluded that $LiMn_{1.5}Ni_{0.5}O_4$ materials with nanorod-shaped morphologies exhibit higher initial discharge capacity and better capacity retention than materials with irregular morphology, irrespective of current rate.

4. Conclusions

$LiMn_{1.5}Ni_{0.5}O_4$ cathode powders were prepared by co-precipitation using oxalic acid. The oxalic acid content efficiently controlled the morphologies and electrochemical properties of the $LiMn_{1.5}Ni_{0.5}O_4$ powders. The nanorod-shaped $LiMn_{1.5}Ni_{0.5}O_4$ cathode powders that were obtained from a high ratio of oxalic acid to metal had higher discharge capacities and better cycling characteristics than did irregularly shaped $LiMn_{1.5}Ni_{0.5}O_4$ powders.

Acknowledgements

This work was supported by a National Research Foundation of Korea grant funded by the Korean government (MEST) (NRF-2009-0092780 and NRF-2009-C1AAA001-0093307) and the Human Resources Development of KETEP grant funded by the Korea government Ministry of Knowledge Economy (No. 20104010100560).

References

[1] D. Guyomard, J.-M. Tarascon, J. Electrochem. Soc. 139 (1994) 222.
[2] T. Ohzuku, R. Brodd, J. Power Sources 174 (2007) 449.
[3] P. Ragupathy, H.N. Vasana, N. Munichandraiah, Mater. Chem. Phys. 124 (2010) 870.
[4] Q.M. Zhong, A. Bonakdarpour, M.J. Zhang, Y. Gao, J.R. Dahn, J. Electrochem. Soc. 144 (1997) 205.
[5] M. Takahashi, T. Yoshida, A. Ichikawa, K. Kitoh, H. Katsukawa, Q. Zhang, M. Yoshio, Electrochim. Acta 51 (2006) 5508.
[6] J.M. Paulsen, J.R. Dahn, Chem. Mater. 11 (1999) 3065.
[7] Y.-K. Sun, K.-J. Hong, J. Prakash, K. Amine, Electrochem. Commun. 4 (2002) 344.
[8] T.-F. Yi, Y.-R. Zhu, R.-S. Zhu, Solid State Ionics 179 (2008) 2132.
[9] H. Wu, Ch.V. Rao, B. Rambabu, Mater. Chem. Phys. 116 (2009) 532.
[10] D.K. Kim, P. Muralidharan, H.-W. Lee, R. Ruffo, Y. Yang, C. Chan, H. Peng, R. Huggins, Y. Cui, Nano Lett. 8 (2008) 3948.
[11] S.H. Ju, Y.C. Kang, J. Power Sources 178 (2008) 387.
[12] E. Hosono, T. Kudo, I. Honma, H. Matsuda, H. Zhou, Nano Lett. 9 (2009) 1045.
[13] T. Yi, C. Dai, K. Gao, X. Hu, J. Alloys Compd. 425 (2006) 343.
[14] Y. Zhang, H. Cao, J. Zhang, B. Xia, Solid State Ionics 177 (2006) 3303.
[15] T.-F. Yi, X.-G. Hu, J. Power Sources 167 (2007) 185.
[16] T.-F. Yi, Y.-R. Zhu, Electrochim. Acta 53 (2008) 3120.
[17] Y. Sun, Y. Yang, X. Zhao, H. Shao, Electrochim. Acta 56 (2011) 5934.
[18] M.M. Thackeray, W.I.F. David, P.G. Bruce, J.B. Goodenough, Mater. Res. Bull. 18 (1983) 461.
[19] B.D. Cullity, Elements of X-ray Diffraction, 2nd ed., Addison-Wesley, Reading, MA, 1978, p. 102.
[20] M.W. Raja, S. Mahanty, R.N. Basu, J. Power Sources 192 (2009) 618.
[21] M. Jo, Y.K. Lee, K.M. Kim, J. Cho, J. Electrochem. Soc. 157 (2010) A841.
[22] B. Markovsky, Y. Talyossef, G. Salitra, D. Aurbach, H.-J. Kim, S. Choi, Electrochem. Commun. 6 (2004) 821.
[23] H.-K. Song, K.T. Lee, M.G. Kim, L.F. Nazar, J. Cho, Adv. Funct. Mater. 20 (2010) 3818.